Journal of Geointerface, Vol. 4, No. 2, December 2025, pp. 78–93 e-ISSN: 2583-6900

Preliminary geochemical assessment of water from man-made waterways in coastal Andhra Pradesh and its implications for agriculture and public health with a new approach

Siba Sundar Sahu [1], Barri Satyannarayana[2,*], Tarun Koley[2]

[1] *Geological Survey of India, Bhubaneswar, Odisha, 751012, India*
[2] *Geological Survey of India, Hyderabad, Telangana, 500068, India*

ABSTRACT

This hydrogeochemical study examines surface water quality over a 1007 km^2 coastal area with Quaternary marine and fluvial sediments, highlighting the influence of natural and human factors on water chemistry and its spatial variability. Physico-chemical parameters such as Electrical Conductivity (EC), Total Dissolved Solids (TDS), and Total Hardness (TH) exhibit decreasing gradients from inland areas toward the coast, attributed to dilution by rainwater, tidal flushing, and lower mineral content in sandy coastal sediments. Major ion chemistry highlights contrasting water type: inland zones show elevated sodium and chloride concentrations suggestive of both saline water encroachment and evaporative effects of fresh surface water while coastal samples are enriched in calcium and bicarbonate, indicating low saline water influenced by recharge dynamics. Piper and Wilcox diagrams corroborate this spatial variability from saline Na–Cl type in the north to mixed Ca–Mg–HCO type in the south. Trace element concentrations (Fe, Mn, Pb, Ba, Zn) reflect both geogenic sources and localized anthropogenic inputs, including industrial discharge and agricultural runoff. Gibbs diagram shows physico-chemical characteristics of the water in this area is controlled by evaporation and precipitation. A novel Trend Feasibility Map (TFM) was developed to spatially visualize water quality trends and identify direction of suitability for drinking and irrigation. The TFM integrates hydrochemical and geospatial data, offering a practical tool for water resource planning in coastal settings. Overall, the study underscores the necessity of spatial and directional approach to water quality assessments in dynamic coastal environments.

ARTICLE HISTORY
Received: 31 July 2025
Revised: 15 August 2025
Accepted: 20 August 2025

https://doi.org/10.5281/zenodo.16908133

KEYWORDS
Man-made waterways
Hydro-geochemistry
Andhra Pradesh
TFM
Anthropogenic

1. Introduction

Quaternary coastal areas globally exhibit significant changes in water sample geochemistry due to the interplay of sea-level fluctuations, sediment dynamics, and human activities (Distefano et al., 2021). Studies show that groundwater in these regions often displays increasing salinity, altered major ion composition, and isotopic shifts as it approaches the shoreline, primarily from seawater intrusion, rock-water

*Corresponding author. Email: satyannarayana.98@gmail.com (BS), sibasundar427@gmail.com (SSS), tarunkoley72@gmail.com (TK)

interactions, and anthropogenic pressures, as seen in coastal India and other international examples (Du et al., 2015; Kumar et al., 2022; Anders et al., 2014). Water geochemistry in the Godavari River is shaped by basalt weathering in the upper basin, groundwater discharge and carbonate precipitation in the middle reaches, and seawater intrusion in the delta. Major ions and isotopic signatures show strong spatial and seasonal variability, influenced by both natural lithology and human activities such as irrigation and damming (Das et al., 2005; Navasakthi et al., 2023; Srinivas et al., 2011). The Krishna–Godavari (KG) delta, located along the eastern coast of Andhra Pradesh, India, is a vital agrarian and ecological region characterized by its extensive alluvial plains and complex hydrogeological systems (Anjaneyulu et al., 2015). Formed by the confluence of the Krishna and Godavari rivers, the delta comprises quaternary sediments of both fluvial and marine origins, including formations such as Ramachandrapuram, Kaikaluru, Godavari, Goguleru, and Polatitippa, dating back to the Holocene epoch (Rao, 1992). These formations have been shaped by processes like marine transgressions and fluvial deposition, resulting in a diverse lithological framework that significantly influences groundwater and surface water chemistry (Fig. 1; Rao and Subrahmanyam, 2017).

The region's hydrogeochemistry is further influenced by challenges such as seawater intrusion, excessive groundwater extraction, and various anthropogenic pressures. Elevated concentrations of total dissolved solids, sodium, and chloride have been observed in specific areas, suggesting salinization processes driven by both natural and human-induced factors. Additionally, trace elements like iron, manganese, lead, and barium have been detected in concentrations exceeding permissible limits in some groundwater samples, raising concerns about water quality and potential health risks (Rao and Subrahmanyam, 2017; Mondal et al., 2010).

Despite the critical importance of water quality in the KG delta, there is a notable paucity of comprehensive studies focusing on the hydrogeochemical characterization of surface water in this region. While groundwater has been the subject of various investigations, surface water—equally crucial for agriculture, aquaculture, and domestic use—has not been extensively analysed, particularly concerning trace element concentrations and their spatial distribution patterns. This gap in knowledge hampers effective water resource management and the development of strategies to mitigate contamination and salinization.

To address this deficiency, the present study undertakes a detailed hydrogeochemical analysis of surface water samples from the coastal areas of Andhra Pradesh within the KG delta. By examining parameters such as pH, EC, TDS, TH, major ions, and trace elements, the research aims to elucidate the spatial variability and underlying processes influencing water quality. The study employs tools like Piper, Wilcox and Gibbs diagrams to classify water types and assess suitability for various uses. While traditional water quality index maps offer zonal analysis of water quality from large number of data set without considering directional trends, our new tool, TFM, introduces spatial trends with directional information for water quality parameters from limited number of datasets.

Through this comprehensive approach, the study aims to address existing knowledge gaps—such as water quality near the mouth of the KG delta, the importance of a directional approach to water quality, and the impact of man-made water channels widely used for agriculture and aquaculture in the region—by providing valuable insights into the geochemical processes influencing surface water in the KG delta.

2. Geology and geomorphology of study area

The Krishna–Godavari Basin (KG Basin) encompasses the extensive deltaic plain formed by the Krishna and Godavari rivers along India's east coast, in Andhra Pradesh, where these rivers discharge into the Bay of Bengal. The study area lies within the Krishna–Godavari Delta complex of the K–G Basin and dates back to the Holocene. These Quaternary sediments, collectively referred to as the Krishna–Godavari Group, were deposited during the Holocene period and originate from the erosion of the Deccan Traps and Proterozoic gneissic rocks (Pattan et al., 2008).

Geologically, the study area is characterized by Quaternary sediments of both marine and fluvial origin, which are part of the Krishna–Godavari Group and date to the Holocene period. Within this group, the Ramachandrapuram and Kaikaluru formations are assigned to the Early Holocene, while the Godavari, Goguleru, and Polatitippa formations correspond to the Late Holocene (Pradhan, 1988; Rengamannar and Dashora, 1989; Reddy and Singaraju, 1989). The area predominantly features exposures

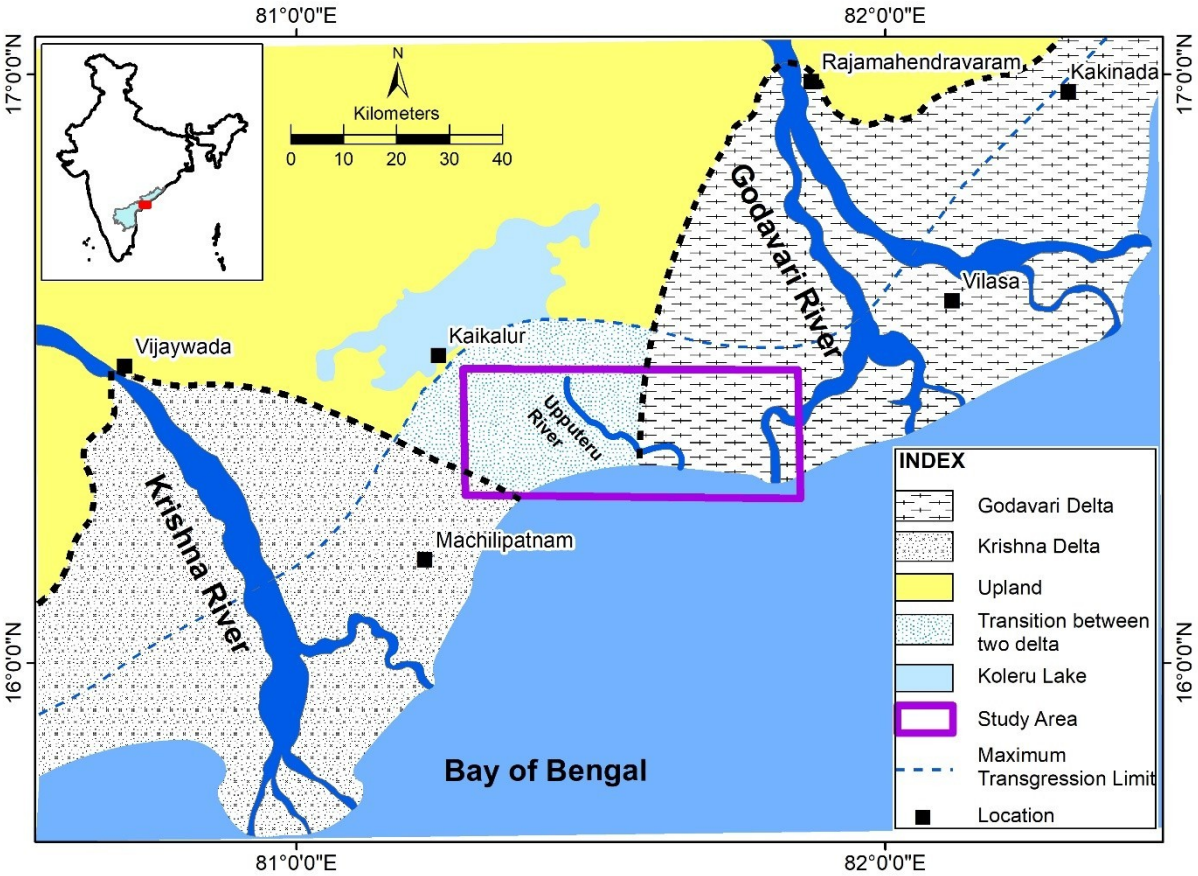

Fig. 1. Regional geomorphological map of Krishna and Godavari delta showing study area (modified after Rao et al., 2013). Inset: Outline map of India showing Andhra Pradesh and deltaic portion.

of Quaternary deposits, including brown silty clay from the Polatitippa Formation and brown fine sand from the Kaikaluru Formation. However, due to widespread anthropogenic activities such as settlement development, agriculture and aquaculture, distinguishing between different lithological units in the field is highly challenging.

The study area lies within a predominantly flat coastal plain near the eastern shoreline of the Krishna–Godavari Basin. It features geomorphic elements such as sand ridges and sandy beaches, characteristic of an older coastal plain setting (Murali et al., 2020; Ramana Murty et al., 1993). The terrain exhibits minimal relief, with elevations ranging from below mean sea level (MSL) to about 36 meters above MSL. Hillshade analysis derived from digital elevation models indicates that the study area is predominantly flat. However, in the southeastern portion near the coast, sand ridges cause a noticeable elevation compared to the surrounding terrain. The study region extends longitudinally from 81°15 E to 81°30 E (covered by SOI toposheet 65H7), and continues up to 81°45 E (within toposheet 65H11). This coastal zone is significantly influenced by the Godavari River and Krishna River, which contribute to the deposition and shaping of Quaternary sediments in the region (Pattan et al., 2008; Gurunadha Rao et al., 2011). These fluvial and deltaic processes are key to the development of the Krishna–Godavari delta complex.

3. Materials and methods

Water samples were collected from 12 locations within the coastal region of Andhra Pradesh from the toposheets 65H7 and 65H11. The sampling area focused on the top half portions of both toposheets, which predominantly feature a network of man-made nalas and canals designed for irrigation and aquaculture purposes. The study area is characterized by alluvial deposits with a gentle coastal gradient, influenced by both fluvial and marine processes. Geologically, the region is composed of recent to sub-recent sediments consisting of sand, silt and clay. The water samples were collected during the post-monsoon

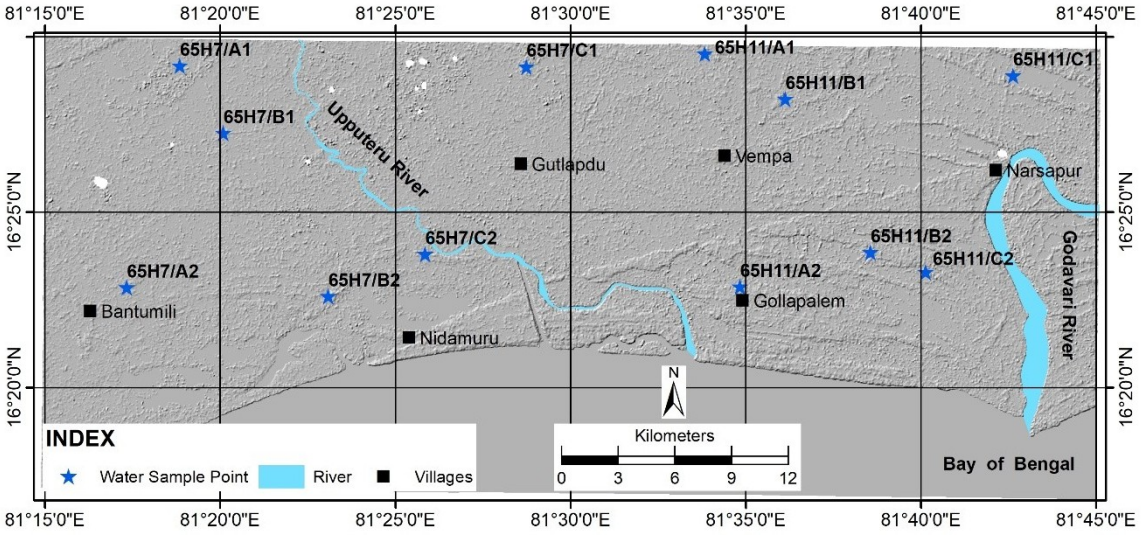

Fig. 2. Hillshade map of the study area showing water sample locations with two natural river Godavari and Upputeru.

period, between August and September 2022, to capture the effects of seasonal recharge and runoff. The 12 sampling locations were systematically designated using a quadrant naming system (A1, B1, C1, A2, B2, C2, etc.), ensuring spatial representation across both toposheets (Fig. 2). A1, B1, C1 of both the toposheet is northern zone of the study area while A2, B2, C2 of both the toposheet is considered as lower half. For sample numbering instead of full name system e.g. 65H07 and 65H11 short form like 7 and 11 is used for ease of reading e.g. 7/A1 instead of 65H07/A1. One quadrant area is bounded by $5' \times 5'$ of a toposheet which is near about 81 km^2. All samples were obtained from surface waters within the canals and nalas, which serve as critical sources for agricultural activities and have potential environmental and health significance.

After collection, the water samples were stored in pre-cleaned, high-density polyethylene bottles, ensuring minimal contamination. Standard procedures recommended by the Geological Survey of India (GSI, 2014) were followed for sample preservation and transportation. Field parameters such as pH, EC, TDS are measured immediately at the site of sampling using portable multi-parameter meters (Table 1). This on-site assessment helps in capturing the real-time physicochemical state of the water before any changes could occur during transport.

For major cation analysis, samples are preserved in the field by acidifying with ultrapure nitric acid (HNO) to maintain a pH of less than 2, while samples meant for anion analysis are kept unacidified and transported under cool conditions. In some cases, filtration using 0.45-micron filters is conducted on-site, especially when the analysis of trace metals is required.

In the laboratory, major cations such as calcium (Ca^{2+}) and magnesium (Mg^{2+}) were determined by titration methods. Sodium (Na^{+}) and potassium (K^{+}) concentrations were measured using a flame photometer (Table 1). Anions like bicarbonate (HCO_3^{-}) and carbonate (CO_3^{2-}) were estimated through acid titration, chloride (Cl^{-}) is determined using the argentometric titration (Mohr's method) and sulphate (SO_4^{2-}) is analysed by chromatography. Nitrate (NO_3^{-}) and fluoride (F^{-}) concentrations were determined using ion-selective electrodes (ISE). For trace metals such as iron (Fe), manganese (Mn), lead (Pb), Barium (Ba) and zinc (Zn), advanced techniques like Inductively Coupled Plasma Mass Spectrometry (ICPMS) was used (Table 2). Instrumental analyses were carefully calibrated using certified standard solutions, and rigorous quality control was maintained by analysing blank samples, duplicate samples, and internal standards.

4. Results

4.1. pH Range

The pH of the water samples varies from 7.2 to 8.1, indicating a slightly alkaline nature for most samples. The lowest pH (7.2) is observed in sample 11/C1, and the highest (8.1) is observed in sample 7/C2 (Table 1). In the study area, the pH values

Table 1. Physicochemical characteristics of surface water samples from the study area, including pH, electrical conductivity (EC), total dissolved solids (TDS), total hardness (TH), major cations (Ca^{2+}, Mg^{2+}, Na^{+}, K^{+}), anions (HCO_3^{-}, Cl^{-}, SO_4^{2-}, NO_3^{-}), and fluoride (F^{-}).

Sample Ref No.	pH	EC (µS/cm)	TDS (ppm)	TH (ppm)	Ca (ppm)	Mg (ppm)	Na (ppm)	K (ppm)	HCO_3 (ppm)	Cl (ppm)	SO_4 (ppm)	NO_3 (ppm)	F (ppm)
65H07/A1	8.0	4910	3192	1050	72	212	429	43	805	1071	23	19	1.89
65H07/B1	8.0	3800	2470	650	80	109	439	22	671	851	21	23	2.00
65H07/C1	7.8	2290	1489	470	80	66	238	17	305	581	13	8	1.80
65H07/A2	7.3	690	449	200	52	17	86	5	317	106	8	12	1.90
65H07/B2	8.0	690	449	220	56	19	92	6	293	128	<5	9	1.80
65H07/C2	8.1	992	645	240	56	24	129	7	305	184	<5	11	1.90
65H11/A1	7.3	1291	839	370	64	51	119	12	305	298	9	12	1.40
65H11/B1	7.3	1488	967	280	56	34	181	10	281	284	11	13	1.70
65H11/C1	7.2	613	398	150	40	24	89	25	195	149	<5	<5	0.09
65H11/A2	7.9	1158	753	250	60	24	149	15	354	227	8	17	1.90
65H11/B2	7.5	284	185	100	28	10	52	21	207	43	<5	<5	0.07
65H11/C2	7.4	275	179	160	40	15	33	<5	207	50	<5	8	1.94

Table 2. Concentrations of trace metals in surface water samples from the study area, including Iron (Fe), Manganese (Mn), Lead (Pb), Barium (Ba) and Zinc (Zn).

Sample Ref No.	Fe (ppb)	Mn (ppb)	Pb (ppb)	Ba (ppb)	Zn (ppb)
65H07/A1	236.65	2.50	5.79	36.41	11.70
65H07/B1	105.03	1.49	1.87	49.71	8.12
65H07/C1	210.33	<0.5	0.74	414.70	3.96
65H07/A2	105.48	8.98	28.68	1124.30	7.38
65H07/B2	114.80	<0.5	1.54	97.74	13.35
65H07/C2	1066.88	0.94	2.56	76.86	26.87
65H11/A1	<100	1.28	1.48	49.95	44.71
65H11/B1	370.59	1.44	2.59	90.79	18.58
65H11/C1	<100	<0.5	<0.5	2434.01	2.87
65H11/A2	134.72	1.31	2.54	1402.52	13.15
65H11/B2	537.31	<0.5	2.38	47.06	9.97
65H11/C2	147.92	0.58	1.78	39.55	40.24

show a decreasing trend from west to east. Most of the sampling points exhibit a curving, inverted S-shaped pattern in pH distribution, indicating a gradual but non-linear change across the region. However, one anomalous sample, located near point A2 of map sheet 65H/7, deviates from this trend and does not conform to the overall spatial pattern (Fig. 3).

4.2. Electrical Conductivity (EC)

The EC ranges from 275 µS/cm to 4910 µS/cm. Sample 7/A1 has the highest EC of 4910 µS/cm, which suggests high dissolved ions in the water. On the other hand, sample 11/C2 has the lowest EC of 275 µS/cm, indicating fewer dissolved ions (Table 1).

4.3. Total Dissolved Solids (TDS)

TDS values range from 179 ppm to 3192 ppm. The highest TDS value (3192 ppm) is observed in sample 7/A1, indicating higher mineralization, while the lowest value (179 ppm) is found in sample 11/C2, suggesting relatively low mineral content (Table 1).

4.4. Total Hardness (TH)

Hardness is measured in ppm, with values ranging from 100 ppm to 1050 ppm. Sample 7/A1 shows the highest hardness (1050 ppm), indicating it has the highest concentration of calcium and magnesium. Samples such as 11/B2 have a lower hardness (100 ppm), indicating soft water (Table 1).

4.5. Ionic concentration

Calcium levels range from 28 ppm to 80 ppm, and magnesium levels vary from 10 ppm to 212 ppm, both contributing to the overall hardness. Sodium concentrations range from 33 ppm to 439 ppm, with the highest concentration found in 7/A1, which may indicate salinity (Table 1). Potassium levels are generally low across the samples, with a maximum of 43 ppm. Bicarbonate (HCO_3) levels range from 43 ppm to 805 ppm, with 7/A1 again showing the highest concentration. Chloride levels range from 43 ppm to 1071 ppm, with the highest value observed in 7/A1, suggesting higher salinity in this sample. Sulphate levels are between 8 ppm and 23 ppm, with 7/A1 again showing

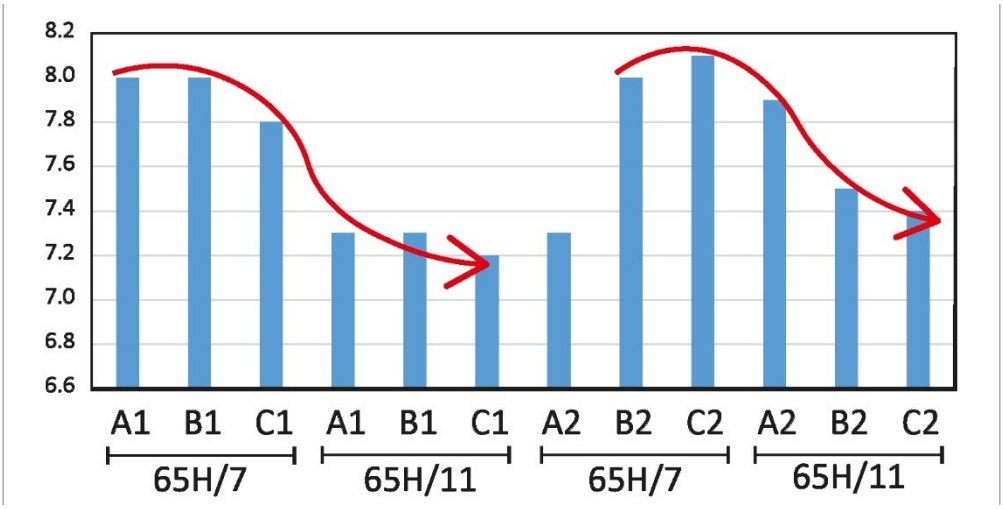

Fig. 3. Bar diagram showing pH values in both the toposheets with trend lines (inverted S shaped red colour line).

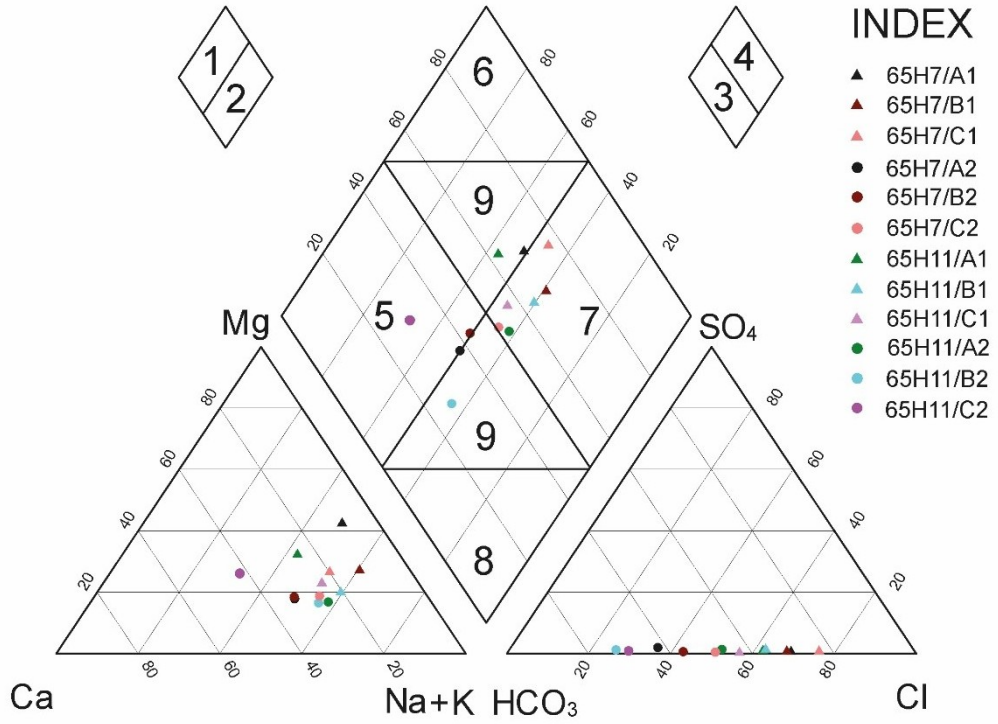

Fig. 4. Piper Diagram water samples based on ion concentrations. Zone 1: Alkaline earth (Ca+Mg) exceeds alkalis (Na+K), Zone 2: Alkalis exceeds alkaline earth, Zone 3: Week acids (CO_3+HCO_3) exceed strong acids (SO_4+Cl), Zone 4: Strong acids exceed week acids, Zone 5: Calcium-Magnesium bicarbonate type, Zone 6: Calcium-Chloride type, Zone 7: Sodium-Chloride type, Zone 8: Sodium bicarbonate type, Zone 9: Mixed type (no cation-anion exceed 50%).

the highest concentration of 23 ppm. Nitrate and phosphate levels are generally low across all samples, with nitrate concentrations mostly under 5 ppm and phosphate levels peaking at 3 ppm in 7/C1. Fluoride concentrations are consistently below 2 ppm in all samples, indicating low fluoride content. Overall, the data suggests that 7/A1 has the highest mineral content and salinity, while 11/B2 is the softest water sample with the lowest hardness and mineral.

While observing the anions (HCO_3^-, Cl^- and SO_4^{2-}) and cations (Ca^{2+}, Mg^{2+}, Na^+ and K^+) in the water sample Piper diagram was prepared which shows a spatial controlled pattern (Piper, 1944). All the samples of northern zone of both the toposheets are falling in zone 2, 4 and 7 while lower half water samples are falling in zone 3, 5 and 9 (Fig. 4). Gibbs diagram was prepared which shows northern zone samples like A1, B1 and C1 of both the toposheet

is falling near to evaporation dominance zone while A2, B2 and C2 are falling in the mixed zone (Fig. 6; Gibbs, 1970).

The Wilcox diagram assesses groundwater suitability for irrigation based on Salinity Hazard (conductivity or TDS) and Sodium Hazard (SAR). Salinity is classified from C1 (low, excellent for irrigation) to C4 (very high, generally unsuitable). Sodium hazard ranges from S1 (low, safe for all soils) to S4 (very high, unsuitable for most crops). Water in C2–C3 and S1–S2 zones is typically usable with proper soil and crop management. The majority of the samples fall within the S1–S2 (Low to Medium Sodium Hazard) and C2–C3 (Medium to High Salinity Hazard) categories, indicating that the sodium levels for irrigation are generally acceptable (Fig. 5). Notably, samples 7/A1 and 7/B1, marked with black and brown triangles, fall within the S2C3 zone, suggesting a medium sodium hazard and a high salinity hazard. This means that the water is marginally suitable for irrigation and demands careful management, particularly in poorly drained soils or for sensitive crops (BIS, 2012). In contrast, samples from the southern region, 11/B2 and 11/C2, fall predominantly within the S1C2 range, indicating low sodium and moderate salinity hazard. These water samples are suitable for irrigation with minimal restrictions (BIS, 2012).

4.6. Trace element concentration

The trace element analysis of the surface water samples shows distinct variability in the concentrations of iron, manganese, lead, barium and zinc. Iron concentrations range widely from below 100 ppb (e.g., in samples 11/A1 and 11/C1) to as high as 1066.88 ppb in sample 7/C2, indicating significant spatial variation (Table 3). Manganese levels are generally low, with most samples registering below 1 ppb or below detection limits (<0.5 ppb), except for sample 7/A2, which shows a relatively high value of 8.98 ppb. Lead concentrations are mostly low, with many samples showing values below 3 ppb; however, sample 7/A2 records the highest concentration of 28.68 ppb. Barium exhibits a broad range of values, from 36.41 ppb in sample 7/A1 to an exceptionally high concentration of 2434.01 ppb in sample 11/C1. Zinc levels range from 2.87 ppb to 44.71 ppb, with the highest concentration found in sample 11/A1. These observations highlight considerable differences in trace element distribution across the sampling locations, with

Table 3. Summary table of ions and trace elements of water samples.

	pH	EC (µS/cm)	TDS (ppm)	TH (ppm)	Ca (ppm)	Mg (ppm)	Na (ppm)	K (ppm)	HCO_3 (ppm)	Cl (ppm)	SO_4 (ppm)	NO_3 (ppm)	F (ppm)	Fe (ppm)	Mn (ppm)	Pb (ppm)	Ba (ppm)	Zn (ppm)
Minimum	7.2	275	178.75	100	28.056	9.728	32.8	2.5	195.264	42.54	2.5	2.5	0.07	0.05	0.0003	0.0003	0.0364	0.0029
Maximum	8.1	4910	3191.5	1050	80.16	211.584	439	43.33	805.464	1070.59	23	23	2	1.067	0.009	0.029	2.434	0.045
Mean	7.65	1540.08	1001.05	345	57.11	50.46	169.67	15.42	353.92	330.87	8.79	11.42	1.53	0.26	0.00	0.00	0.49	0.02
Median	7.65	1075	698.75	245	56.112	24.32	124.2	13.41	305.1	205.61	8	11.5	1.845	0.14132	0.00111	0.00212	0.08383	0.01242
Standard Deviation	0.345	1446.63	940.31	269.60	15.95	58.01	135.24	11.30	188.35	330.69	7.216	6.138	0.696	0.291	0.002	0.008	0.768	0.014
Skewness	0.000	1.58	1.58	1.92	-0.17	2.32	1.38	1.37	1.84	1.46	1.024	0.310	-1.854	2.283	2.985	3.284	1.863	1.247
Kurtosis	-2.024	1.81	1.81	3.81	-0.38	5.63	0.91	2.42	2.64	1.18	0.102	-0.121	2.058	5.566	9.543	11.051	2.950	0.520
Count	12	12	12	12	12	12	12	12	12	12	12	12	12	12	12	12	12	12

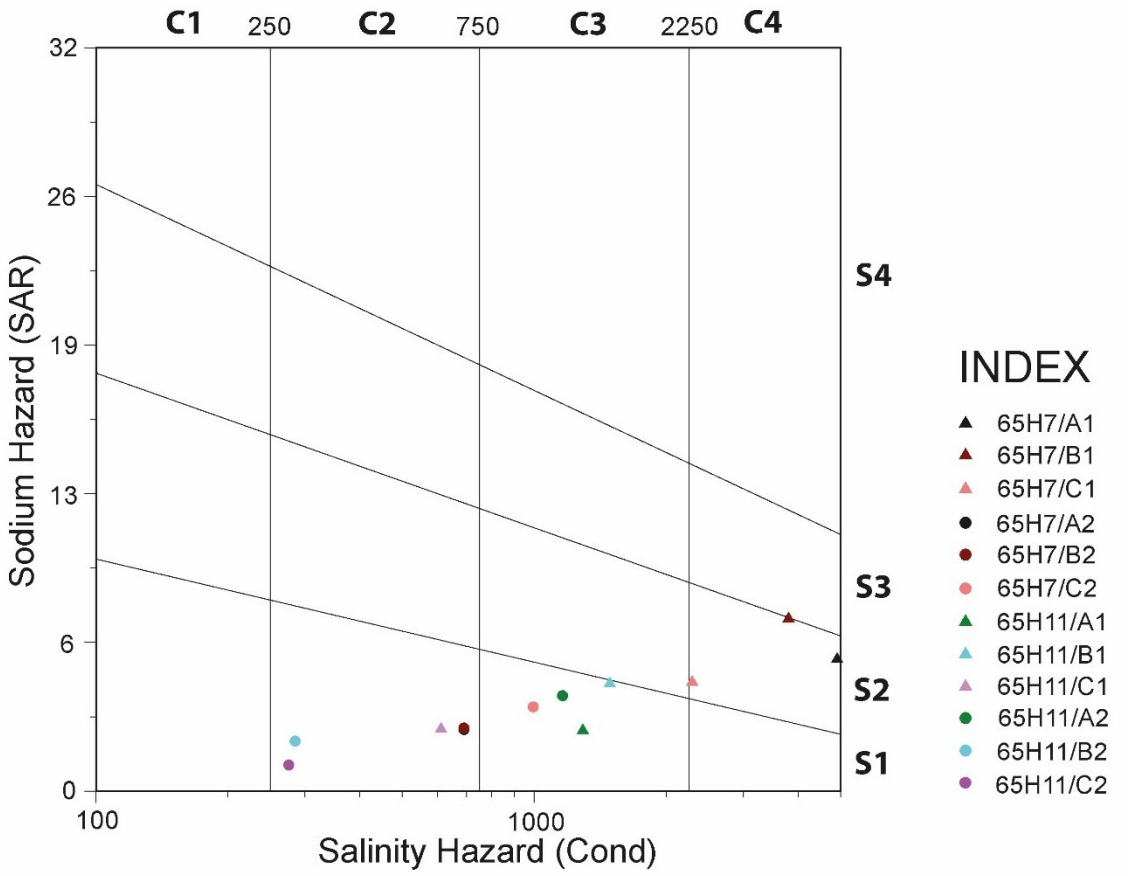

Fig. 5. Wilcox diagram illustrating the classification of irrigation water quality based on sodium hazard (SAR) and electrical conductivity (EC) for the analysed water sample.

certain sites exhibiting markedly elevated concentrations of specific metals.

5. Interpretation

5.1. pH:

Surface water in this coastal region exhibits a slightly alkaline pH primarily due to natural geochemical processes. The dissolution of carbonate minerals such as calcite and dolomite—common in coastal aquifers—releases bicarbonate ions, enhancing alkalinity and contributing to pH stabilization (Hem, 1985). Additionally, interaction between coastal groundwater and seawater, which naturally has a higher pH (around 8.1–8.3), elevate surface water pH, particularly during dry seasons (Langmuir, 1997). Anthropogenic influences also contribute to this alkaline environment. Agricultural runoff and effluent discharges introduce lime or bicarbonate-rich materials, such as fertilizers or construction waste, further raising pH levels. During dry periods, limited freshwater recharge leads to the concentration of these ions, amplifying the buffering capacity and sustaining alkaline conditions (Custodio and Bruggeman, 1987). Elevated concentrations of total dissolved solids and electrical conductivity, mainly due to sodium, chloride and bicarbonate ions, reinforce this stability (Freeze and Cherry, 1979).

5.2. EC and TDS

The EC varies with minimum value of 275 to maximum value 4910 µS/cm (Table 3). EC is a measure of the water's ability to conduct electricity, related to the concentration of dissolved salts. Values above 1500 µS/cm indicate high salinity, which may limit the water's suitability for irrigation and sometimes for drinking (Table 5; BIS, 2012). Samples like 7/A1 with EC close to 5000 µS/cm suggest very high salinity, pointing toward possible saline contamination or natural mineral dissolution. TDS values range from 179 ppm to 3192 ppm. TDS below 500 ppm is considered excellent for drinking, while values above 1500 ppm are unsuitable for human consumption without treatment (Table 5; BIS, 2012). Hence, samples like

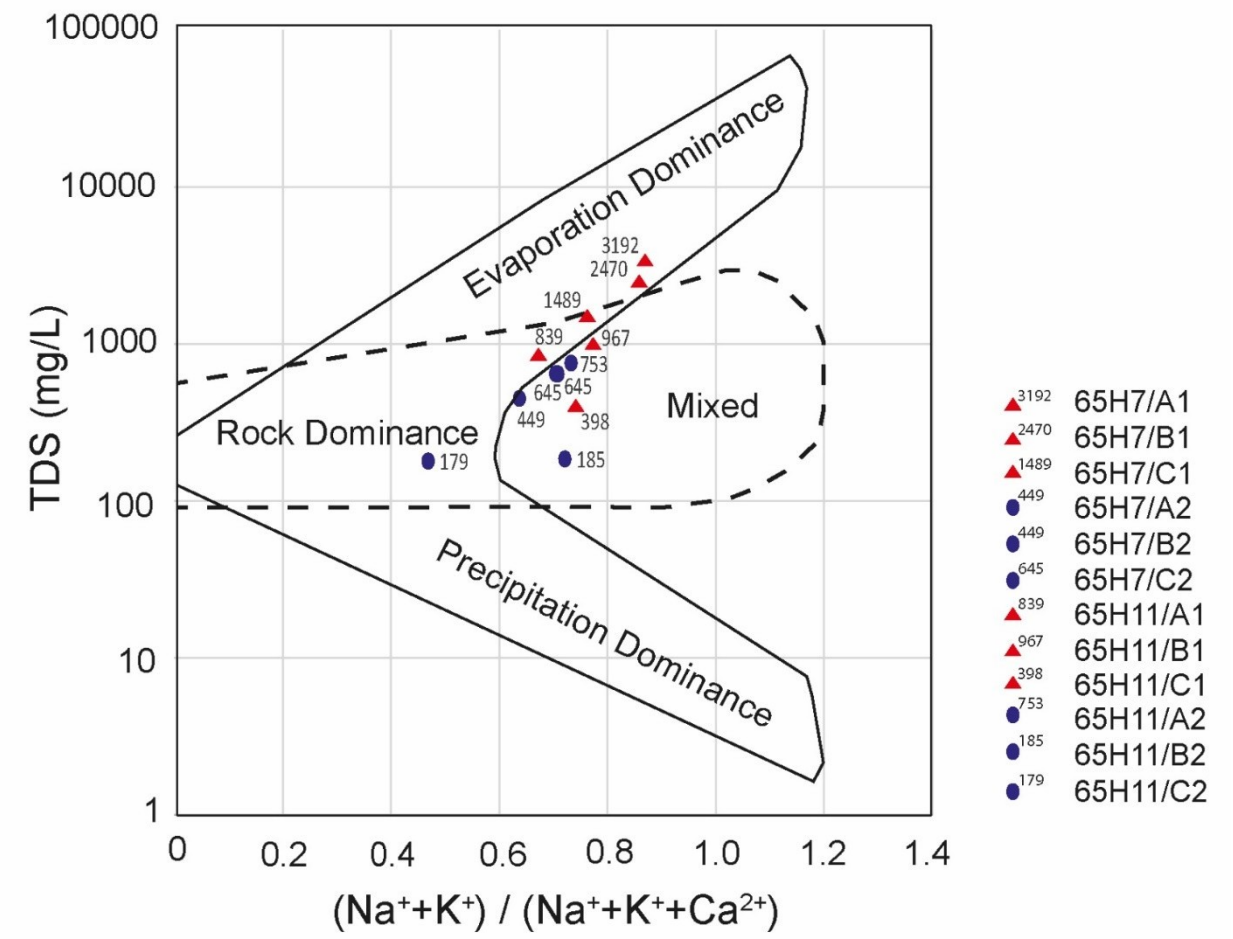

Fig. 6. Gibb's bivariate diagram showing evaporation vs precipitation concentration of water samples.

7/A1 (3192 ppm) indicate highly mineralized water, possibly not fit for drinking. While EC and TDS are correlated, they are distinct parameters that exhibit similar spatial trends like both decreases towards coast line. This happens because of two reasons i.e. anthropogenic barriers like lots of pondlike structure which hold fresh water for irrigation and fish culture prevent saline water intrusion. Here in this area the water from that reserve get mixed to the man-made canals and also receive water from this which cause frequent mixing of water cause dilution of riverine TDS.

5.3. TH

Values of TH decreases from 1050 ppm in 7/A1 to 100 ppm in 11/B2. A gradual decreasing EC and TH towards coast has been observed in the water samples. This is due to dilution by fresher water sources like rainwater and surface runoff. Coastal sediments are mainly sandy and less mineral-rich compared to inland formations, resulting in reduced water-rock interaction and lower dissolution of hardness-causing minerals. Frequent tidal flushing and shorter groundwater residence time near the coast also limit salt accumulation, further contributing to the observed decrease in EC and TH values. Calcium and Magnesium concentrations are also significant. Calcium values between 28 ppm and 80 ppm are common, where higher concentrations (>75 ppm) like in 7/B1 may contribute heavily to hardness. Magnesium values are very high in some samples, notably 212 ppm in 7/A1, which is quite elevated compared to the WHO (1996) guideline of 50 ppm for drinking water (Table 6). High magnesium concentrations can cause a laxative effect if consumed regularly.

5.4. Ionic concentration

Sodium levels are especially high (up to 439 ppm). For drinking purposes, sodium concentration should preferably be below 200 ppm. Excess sodium can cause taste issues and health concerns, especially for people with hypertension. Samples exceeding 200

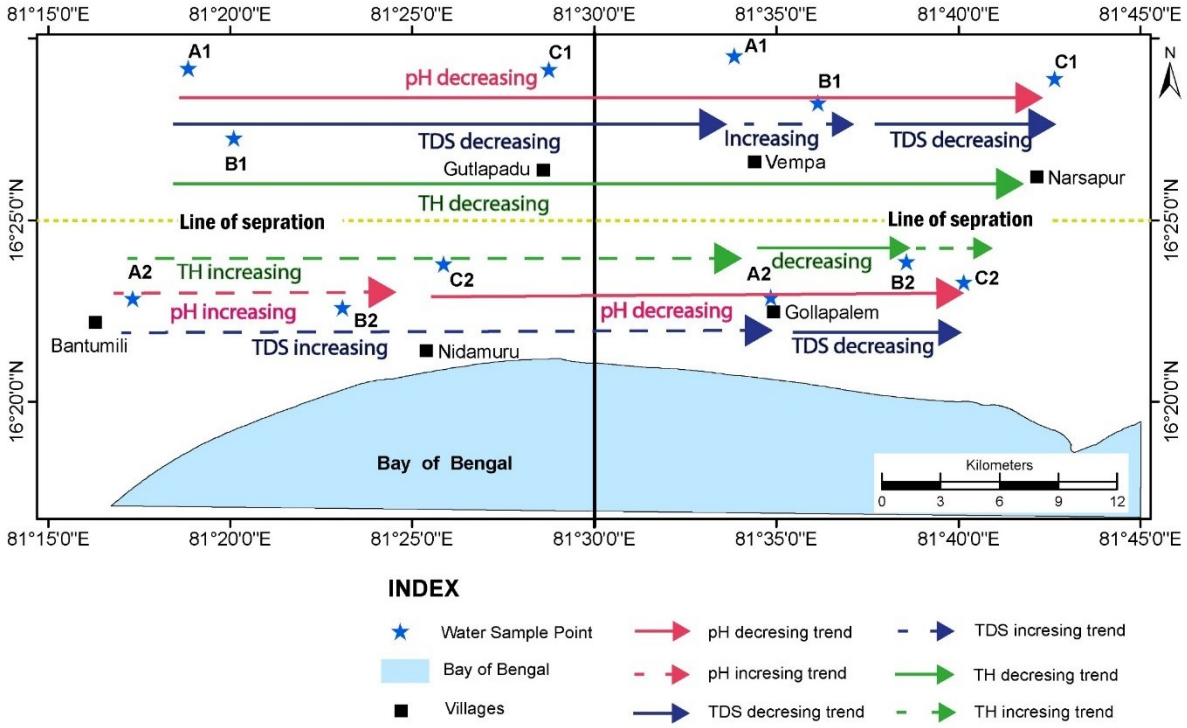

Fig. 7. Trend Feasibility Map (TFM) depicting the spatial trends of pH, electrical conductivity (EC), and hardness in water samples, highlighting zones of increasing or decreasing water quality.

ppm (like 7/A1, 7/B1) would be unsuitable without treatment (Table 5). Potassium values remain relatively low (<50 ppm), within safe and normal natural ranges. Potassium at these levels does not pose a health risk. Carbonate is absent (ND = not detected) in all samples, but bicarbonate values range from 195 to 805 ppm. High bicarbonate concentrations indicate a good buffering capacity, but also hint at the possibility of alkalinity-related issues in irrigation waters, especially when paired with high sodium. Chloride values vary from 43 to 1071 ppm. Chloride above 250 ppm can make the water taste salty and is a marker for possible contamination from saltwater intrusion, sewage, or agricultural runoff. Samples exceeding this, like 7/A1, indicate potential non-potability. Sulphate levels are moderate, with a maximum of 23 ppm, which is well within safe drinking limits (<250 ppm according to WHO (1996) standards). No sulphate-related problems are indicated. Nitrate concentrations are low across the samples (<13 ppm). Nitrate levels below 45 ppm are considered safe for drinking. Thus, there is no immediate risk of agricultural pollution or sewage contamination here. Phosphate concentrations are very low (generally <2 ppm), indicating minimal agricultural fertilizer contamination or industrial pollution. Fluoride (F^-) concentrations are mostly below 2 ppm, with the highest being 2 ppm in 7/B1. According to WHO (1996) guidelines, the fluoride limit is 1.5 ppm; therefore, slightly elevated fluoride may pose a risk of dental fluorosis if consumed over the long term (Table 5).

5.5. Correlation coefficient (r) between ions

A correlation matrix prepared for all physicochemical properties (Table 4) reveals very strong (green, r 0.90) and strong (orange, r 0.80) correlations between the measured parameters. Notably, total hardness (TH), total dissolved solids (TDS), and electrical conductivity (EC) exhibited exceptionally high correlation coefficients (r = 0.98–0.99). While a strong correlation between TDS and EC is expected, the similarly high correlation with TH suggests that water hardness is predominantly influenced by the concentration of dissolved solids. Furthermore, both cations and anions in the water samples demonstrated strong correlations (r 0.90), consistent with the principle of electroneutrality, which dictates that the total positive and negative charges in a solution must be balanced. These findings indicate that the ions contributing to hardness and alkalinity likely originate

Table 4. Correlation coefficient between the physico-chemical properties of water sample.

	pH	EC (µS/cm)	TDS (ppm)	TH (ppm)	Ca (ppm)	Mg (ppm)	Na (ppm)	K (ppm)	HCO_3 (ppm)	Cl (ppm)	SO_4 (ppm)	NO_3 (ppm)	F (ppm)	Fe (ppm)	Mn (ppm)	Pb (ppm)	Ba (ppm)	Zn (ppm)
pH	1																	
EC	0.50	1																
TDS	0.50	1.00	1															
TH	0.48	0.98	0.98	1														
Ca	0.54	0.77	0.77	0.74	1													
Mg	0.43	0.96	0.96	0.99	0.64	1												
Na	0.54	0.98	0.98	0.92	0.80	0.89	1											
K	0.23	0.74	0.74	0.74	0.28	0.81	0.69	1										
HCO_3	0.56	0.95	0.95	0.94	0.68	0.93	0.93	0.69	1									
Cl	0.49	1.00	1.00	0.97	0.79	0.95	0.98	0.75	0.92	1								
SO_4	0.34	0.96	0.96	0.92	0.79	0.89	0.95	0.65	0.90	0.95	1							
NO_3	0.51	0.74	0.74	0.69	0.73	0.63	0.78	0.27	0.82	0.70	0.79	1						
F	0.49	0.39	0.39	0.40	0.65	0.29	0.39	-0.26	0.43	0.36	0.42	0.71	1					
Fe	0.35	-0.12	-0.12	-0.14	-0.19	-0.14	-0.11	-0.13	-0.12	-0.15	-0.26	-0.14	-0.02	1				
Mn	-0.23	0.04	0.04	0.06	0.05	0.04	0.01	-0.13	0.17	-0.01	0.19	0.27	0.29	-0.17	1			
Pb	-0.25	-0.08	-0.08	-0.05	-0.07	-0.06	-0.11	-0.18	0.06	-0.12	0.06	0.12	0.22	-0.12	0.98	1		
Ba	-0.36	-0.28	-0.28	-0.32	-0.25	-0.27	-0.25	0.11	-0.28	-0.27	-0.26	-0.28	-0.41	-0.34	0.18	0.19	1	
Zn	-0.19	-0.25	-0.25	-0.15	-0.13	-0.17	-0.32	-0.45	-0.21	-0.26	-0.25	0.01	0.24	0.12	-0.17	-0.21	-0.46	1

from a common source. Collectively, these relationships suggest that the same set of ions is responsible for increasing water hardness, alkalinity, and conductivity, primarily through their presence as dissolved solids.

5.6. Interpretive diagrams

The Piper diagram reveals a clear spatially controlled geochemical pattern that aligns with the division of the study area into northern and southern zones (Fig. 4). These samples predominantly plot in fields 2, 4, and 7, indicating alkali ($Na^+ + K^+$) dominance over alkaline earths ($Ca^{2+} + Mg^{2+}$) and strong acid ($Cl^- + SO_4^{2-}$) dominance over weak acids (HCO_3^-), thus classifying the water type as sodium-chloride (NaCl) or saline (Tarawneh et al., 2019; Xu et al., 2023). This geochemical characteristic suggests influence from marine or coastal processes, saline intrusion, or evaporative concentration, particularly in areas closer to the coastline or with reduced fresh water recharge. Lower half samples fall in fields 3, 5, and 9, reflecting alkaline earth dominance, Weak acid dominance (Fig. 4). Water type is Mixed or Ca–Mg–HCO type. This indicates low saline and bicarbonated groundwater, often associated with recharge zones, less mineralized environments, or carbonate-rich aquifers. The presence of mixed-ion points to water-rock interaction and less saline influence. The observed water types and its transitions are likely influenced by multiple factors. These factors are geological controls, distance from coastline, recharge-discharge dynamics and anthropogenic impacts. The proximity of the northern zone to the sea increases the chance of saline influence and marine aerosol input. The southern zone possibly acts as a recharge area with more active flushing and less evaporative concentration. This interpretation supports the spatial differentiation of groundwater quality shown in the TFM and aligns with other parameters such as TDS and hardness, which also vary systematically across the landscape (Fig. 7). This reflection of less evaporation and a mixed environment in southern part samples come clearly in TDS vs alkali in Gibbs bivariate diagram (Fig. 6). Gibbs bivariate diagram shows the effect of precipitation and evaporation which is calculated from two parameters i.e. TDS and alkali (Gibbs, 1970). Water physico-chemical character is not influenced by lithology in this study area rather it is combined effect of rainfall and evaporation process. Additional to this besides being placed

Table 5. Feasibility Index table for anions and cations w.r.t. to drinking water and irrigation water (after BIS IS 10500, 2012; Central Pollution Control Board (CPCB), 2008 and Ayers and Westcot, 1985).

		Drinking Index		Irrigation Index	Remarks
		Class 1	Class 2	Class 1	
pH	Range	6.5–8.5	<6.5 and >8.5	6.5–8.5	All the samples are within permissible limit
	N	12	0	12	
TDS	Range	<500	500–2000	<2000	Two samples i.e. 65H07/A1 and B1 is having more TDS than permissible limit
	N	5	5	10	
TH	Range	<200	200–600	<600	Two samples i.e. 65H07/A1 and B1 is having more TH than permissible limit
	N	4	6		
Ca	Range	<75	75–200	<200	All the samples are within permissible limit
	N	10	2	12	
Mg	Range	<30	30–100	<100	Two samples i.e. 65H07/A1 and B1 is having more Mg than permissible limit
	N	7	3		
Na	Range	NA	NA	<200	Three samples i.e 65H07/A1, B1 and C1 are above the permissible limit
	N	-	-	9	
K	Range	NA	NA	<10	Seven samples having more than the permissible limit for irrigation purpose
	N	-	-	5	
HCO_3	Range	NA	NA	NA	NA
	N	-	-		
Cl	Range	<250	250–1000	<1000	One sample i.e. 65H07/A1 is having more Cl than permissible limit
	N	7	4	11	
SO_4	Range	<200	200–400	<400	All the samples are within permissible limit
	N	12	0	12	
NO_3	Range	<45	No relaxation	<45	All the samples are within permissible limit
	N	12	0	12	
F	Range	<1.0	1.0–1.5	<1.5	Rest all the 09 samples are above the limit but within 2 ppm
	N	2	1	3	

at the Krishna and Godavari delta portion which have flown over various lithologies of Peninsular India the water does now follow any of the lithological trend. This shows the manmade waterways are generated in a closed system or partially connected to these two rivers which doesn't allow to intermix with the lithological variation.

Wilcox diagram shows northern samples (top half of toposheets) tend to show higher salinity and sodium levels (S2C2 to S2C3), potentially due to proximity to coast, marine influence, or lower recharge rates. Southern samples (lower half) are generally in safer zones (S1C2), making them more suitable for sustained agricultural use (Fig. 6). Management Implication: In areas with S2C3 classification, farmers should consider soil conditioning, salt-tolerant crops, and irrigation techniques that minimize salt buildup.

5.7. Trace elements concentration

The trace element concentration variations across the surface water samples suggest a combination of geogenic and anthropogenic influences (Indugula and Venkata Vajjha, 2023). Elevated iron concentration, particularly in sample 7/C2, may result from natural weathering of iron-rich minerals or localized input from anthropogenic sources such as corroded infrastructure. The generally low manganese levels imply oxidizing environmental conditions, with the exception of the high value in 7/A2, which could indicate localized reducing environments or mineral dissolution. The significantly high lead concentration in 7/A2 suggests possible contamination from industrial or urban sources, as lead is not commonly abundant in natural water systems without external input. A very strong correlation was observed between Mn and Pb ($r = 0.98$), suggesting a link to the aquaculture feeds (Table 4). Since Mn is an essential micronutrient for fish growth, it appears that Pb is also present in these feeds. This indicates that fish feed is likely produced from common sources containing both Mn and Pb. Even study shows fish feeds and fish farms use these trace elements unintentionally but regular use cause accumulation as observed in some of the water sample in this area where extensive aqua culture activity occurs (Mannzhi et al., 2021).

Table 6. Feasibility Index table for anions and cations w.r.t. to irrigation water (after BIS, 1998).

		Drinking Index		Irrigation Index	Remarks
		Class 1	Class 2	Class 1	
Fe	Range	1	No relaxation	NA	One sample i.e. 65H07/C2 above the permissible limit
	N	11	1	-	
Mn	Range	<0.1	0.1–0.3	NA	All the samples are within permissible limit
	N	12	0	-	
Pb	Range	<0.1	No relaxation	NA	All the samples are within permissible limit
	N	12	0	-	
Ba	Range	<0.7	No relaxation	NA	Three samples i.e 65H07/A2 and 65H11/C1 and A2 are above the accepted limit
	N	9	3	-	
Zn	Range	<5	5–15	NA	All the samples are within permissible limit
	N	12	0	-	

The extreme barium concentrations, particularly in samples 11/C1 and 11/A2, may originate from manufacturing discharge or agricultural runoff (Maurya et al., 2019). Zinc levels are generally moderate, but the highest concentration in 11/A1 may reflect contamination from agricultural runoff, vehicular traffic or waste disposal activities. Skewness of all the trace elements are high indicating water flown over a mixed environment where specific lithology signature is not preserved (Table 3). Overall, the spatial distribution patterns of these trace elements point to localized sources of contamination and underscore the importance of further investigation to distinguish between natural and anthropogenic contributions to water quality in the study area.

6. Trend Feasibility Map (TFM): A new spatial approach to water quality

In a study area covering approximately 1007 km^2, encompassing two toposheets, various physicochemical parameters such as pH, TDS, EC, salinity, and hardness were analysed. While the parameters initially displayed a wide range of values, a closer spatial examination revealed a distinct trend influenced by the distance from the coastline both longitudinally and latitudinally, reflecting spatial variations. This spatial pattern exhibited a consistent gradient across most water quality parameters, with concentrations either increasing or decreasing proportionally with distance from the coastline (Table 6). The direction and magnitude of these gradients demonstrated a clear correlation between coastal proximity and water quality, directly influencing the suitability of water for both drinking and irrigation purposes. Based on the sample values and their comparison with national standards, the suitability of water for drinking has been assessed. Accordingly, two suitability classes were defined based on their accepted and permissible limits: Class 1 (high suitability), Class 2 (low suitability). In case of irrigation only permissible limit was considered (BIS, 1998). To better visualize the spatial distribution of water quality, a novel conceptual mapping technique referred to as the Trend Feasibility Map has been introduced, offering an intuitive representation of regional trends in water suitability (Fig. 7). The TFM synthesizes analysed water quality data into a simplified, visually interpretable format that highlights gradient directions and their correlation with coastal distance. This tool offers valuable insights into water suitability across the landscape and serves as a practical framework for future research and planning in coastal and peri-coastal regions. Water Quality Index (WQI) is another way for spatial analysis of water quality but demands a greater number of samples (Horton, 1965). But, in TFM method small number of samples could be presented spatially.

The study area is longitudinally aligned, extending from toposheet 65H/07 on the left to 65H/11 on the right, and is divided into 5 ×5 quadrants labelled A, B, and C. An interpreted ”line of separation” demarcates the northern and southern zones, indicating a possible hydrological boundary that influences the region’s water chemistry. In terms of pH trends, the northern zone shows a decreasing pattern from west to east, while the southern zone generally shows an increasing trend. However, the pH values remain within the safe range for drinking water, as per BIS (2012) guidelines—ranging from 7.2 to 8.0 in the north and 7.3 to 8.1 in the south (Fig. 7). Similarly, TDS values range from 398 to 3192 ppm in the northern region and from 179 to 753 ppm in the southern region. In the northern part, samples from quadrants A1 and B1 of map sheet 65H/07 fall within the moderate range for drinking water, with only a slight impact

on taste. Despite the higher TDS values, the water remains suitable for irrigation with minimal effect on crops (BIS, 2012). In the southern region, all samples fall within the low to moderate range, making the water suitable for both drinking and irrigation, with only a slight alteration in taste (Fig. 7). In the northern region, TH values range from 150 to 1050 ppm, while in the southern region they range from 100 to 250 ppm. For irrigation purposes, all samples fall within the safe range. However, for drinking purposes, most samples are within the moderately hard category. An exception is the sample from quadrant A1 of map sheet 65H/07, which has a TH value of 1050 ppm. This makes the water very hard, resulting in poor taste and potential scaling issues.

In terms of feasibility, the pH values of all water samples exhibit a decreasing trend from west to east in both the northern and southern regions. These values remain within a range that is generally considered safe for both health and irrigation purposes. The TDS level decrease from west to east in the northern region, whereas they increase in the southern region. In the north, higher TDS levels are likely due to the mixing of multiple environmental factors and the distance from seawater, which may pose health risks. In contrast, the southern region contains a moderate level of dissolved solids, presenting fewer health concerns. From an irrigation standpoint, TDS levels do not pose any significant issues. TH displays a decreasing trend from west to east in the northern region, while it increases in the southern region. In terms of feasibility, water in both regions may require slight treatment to be fully suitable for drinking and irrigation.

7. Conclusions

The hydrogeochemical investigation of the coastal study area reveals a complex interplay of geological, hydrological and anthropogenic factors influencing surface water quality which exhibits distinct spatial variability in its water chemistry from the following conclusions.

1. Physico-chemical parameters such as EC, TDS and TH display clear spatial gradients, generally decreasing from inland regions toward the coast. These trends reflect both natural dilution by rainwater and surface runoff, and the influence of less mineralized, sandy coastal sediments. While certain inland samples i.e. 7/A1 and 7/B1 exhibit elevated salinity and mineral content, potentially rendering them unsuitable for drinking, the overall water quality remains within acceptable limits for irrigation in most areas (Table 5).
2. Elevated sodium and chloride concentration in some northern samples indicate possible evaporative concentration. Conversely, southern samples with higher proportions of calcium and bicarbonate suggest active recharge zones with limited salinization. This spatial transition in water types—from Na–Cl to Ca–Mg–HCO mixed type—is supported by both Piper and Wilcox diagrams, indicating a shift from saline to less saline water chemistry across the study area.
3. Gibbs bivariate diagram shows all the salinity regrading issue is not from the lithology rather from evaporation and precipitation phenomena.
4. Trace element analysis confirms the influence of both natural and anthropogenic sources. Elevated concentrations of iron, lead, barium, and zinc in certain samples point to localized contamination and agricultural runoff. While most trace metals remain within permissible limits, a few samples i.e. 28.68 ppb of Pb in 7/A2 and 2434.01 ppb of Ba in 11/C1 which exceed recommended thresholds, underscoring the need for continuous monitoring.
5. To visualize and manage this spatial heterogeneity in water quality, the development of TFM has proven highly effective. From this a quick visualization come out like pH is decreasing from west to east. TDS is decreasing from west to east in the northern and increasing from west to east in the southern part. TH is decreasing from west to east in the northern part and increasing in the southern part.
6. In conclusion, it is observed that patterns are influenced by seawater proximity and anthropogenic pressures. Distance from the coast became a major factor in controlling the chemical concentration of water. Extensive irrigation and fish culture with additional factor of evaporation and precipitation activity reverse the trend of salinity and bicarbonate concentration in the surface water. Rainfall and fresh water interaction in the coastal part make the water less saline while water away from the coast affected by anthropogenic activity extensively

which make it more saline. Overall, these combined natural and anthropogenic factors create a chemically stable water environment that is non-aggressive toward plumbing infrastructure and generally safe for aquatic ecosystems.

Acknowledgements

We sincerely extend our heartfelt gratitude to the Additional Director General (ADG) and Head of Department (HOD) of the Geological Survey of India (GSI), Southern Region (SR), Hyderabad, as well as the Deputy Director General (DDG) of the Regional Mission Head, GSI, SR, and the DDG, State Unit Andhra Pradesh, GSI, SR, Hyderabad, for their generous support and for providing the necessary resources essential for the successful execution of this Field Season Programme.

CRediT statement

SSS: Conceptualization, Investigation, Methodology, Data generation, Writing – review & editing. **BS:** Investigation, Methodology, Data generation, Writing & editing, corresponding author. **TK:** Writing – review, editing, supervision.

Conflict of Interest

The authors declare that they have no known competing financial interests or personal relationships that could have appeared to influence the work reported in this paper.

References

Anders, R., Mendez, G.O., Futa, K., Danskin, W.R., 2014. A geochemical approach to determine sources and movement of saline groundwater in a coastal aquifer. *Groundwater* 52(5), 756–768. https://doi.org/10.1111/gwat.12108.

Anjaneyulu, K., Vijay Durga, N., Sandip, B., Sathish, G., Vairavan, R.V., Banerjee, D., Meetei, L.I., Borkar, B.N., 2015. Morphology and structure of Godavari sub-aqueous delta and adjoining continental margin, East Coast of India. *Indian Journal of Geosciences* 69(3&4), 203–214.

Ayers, R.S., Westcot, D.W., 1985. *Water Quality for Agriculture. FAO Irrigation and Drainage Paper 29 Rev. 1.* Rome: Food and Agriculture Organization of the United Nations. URL: https://www.fao.org/3/t0234e/t0234e00.htm. available online:.

BIS, 1998. *Drinking Water Specifications (revised 2003).* Bureau of Indian Standards, IS:10500.

BIS, 2012. *IS:10500:2012 Indian Standard Drinking Water–Specification.* 2nd revision. Bureau of Indian Standards, New Delhi.

Central Pollution Control Board (CPCB), 2008. *Guide Manual: Water and Wastewater Analysis.* Ministry of Environment, Forest and Climate Change, Government of India, New Delhi.

Custodio, E., Bruggeman, G.A., 1987. *Groundwater Problems in Coastal Areas.* UNESCO. URL: https://coilink.org/20.500.12592/ghx3jc0.

Das, A., Krishnaswami, S., Sarin, M.M., Pande, K., 2005. Chemical weathering in the Krishna and Godavari River basins: Weathering controls and CO_2 consumption. *Geochimica et Cosmochimica Acta* 69(8), 2067–2084. https://doi.org/10.1016/j.gca.2004.10.014.

Distefano, S., Gamberi, F., Borzì, L., Stefano, A., 2021. Quaternary coastal landscape evolution and sea-level rise: An example from South-East Sicily. *Geosciences* 11(12), 506. https://doi.org/10.3390/geosciences11120506.

Du, Y., Ma, T., Chen, L., Shan, H., Xiao, C., Lu, Y., Liu, C., Cai, H., 2015. Genesis of salinized groundwater in Quaternary aquifer system of coastal plain, Laizhou Bay, China: Geochemical evidences, especially from bromine stable isotope. *Applied Geochemistry* 59, 155–165. https://doi.org/10.1016/j.apgeochem.2015.04.017.

Freeze, R.A., Cherry, J.A., 1979. *Groundwater.* Prentice-Hall.

Gibbs, R.J., 1970. Mechanisms controlling world water chemistry. *Science* 170(3962), 1088–1090. https://doi.org/10.1126/science.170.3962.1088.

GSI, 2014. Standard Operating Procedure for National Geochemical Mapping & Quality Management GSI. Mission-1.

Gurunadha Rao, V.V.S., Rao, G.T., Surinaidu, L., Rajesh, R., Mahesh, J., 2011. Geophysical and geochemical approach for seawater intrusion assessment in the Godavari Delta Basin, AP, India. *Water, Air, & Soil Pollution* 217, 503–514. https://doi.org/10.1007/s11270-010-0604-9.

Hem, J.D., 1985. *Study and Interpretation of the Chemical Characteristics of Natural Water.* 3rd ed., U.S. Geological Survey Water-Supply Paper 2254.

Horton, R.K., 1965. An index number system for rating water quality. *J Water Pollut Control Fed* 37(3), 300–306.

Indugula, R., Venkata Vajjha, H., 2023. Spatial variations of trace metals, salinization processes and multivariate analysis in the near surface aquifer systems of Krishna delta. *Andhra Pradesh, India. Environmental Earth Sciences* 82(10), 246. https://doi.org/10.1007/s12665-023-10910-6.

Kumar, P., Biswas, A., Banerjee, S., Rathore, S., Rana, V., Ram, K., Acharya, T., 2022. Integrating magnetic susceptibility, hydrogeochemical, and isotopic data to assess the seawater invasion in coastal aquifers of Digha, West Bengal, India. *Environmental Science and Pollution Research* , 1–30https://doi.org/10.1007/s11356-021-16934-4.

Langmuir, D., 1997. *Aqueous Environmental Geochemistry.* Prentice Hall.

Mannzhi, M.P., Edokpayi, J.N., Durowoju, O.S., Gumbo, J., Odiyo, J.O., 2021. Assessment of selected trace metals in fish feeds, pond water and edible muscles of Oreochromis mossambicus and the evaluation of human health risk associated with its consumption in Vhembe district of Limpopo Province, South Africa. *Toxicology Reports* 8, 705–717. https://doi.org/10.1016/j.toxrep.2021.03.018.

Maurya, P.K., Malik, D.S., Yadav, K.K., Kumar, A., Kumar, S., Kamyab, H., 2019. Bioaccumulation and potential sources of heavy metal contamination in fish species in River Ganga basin: Possible human health risks evaluation.

Toxicology Reports 6, 472–481. https://doi.org/10.1016/j.toxrep.2019.05.012.

Mondal, N.C., Singh, V.S., Puranik, S.C., Singh, V.P., 2010. Trace element concentration in groundwater of Pesarlanka Island, Krishna Delta, India. *Environmental Monitoring and Assessment* 163(1-4), 215–227. https://doi.org/10.1007/s10661-009-0828-6.

Murali, R.M., Reshma, K.N., Kumar, S.S., Balaji, S.A., Krishnam Raju, D.M., Ramakrishnan, R., 2020. Spatio-temporal coastal morphological changes of Godavari delta region in the east coast of India. *Journal of Coastal Research* 95(SI), 626–631. https://doi.org/10.2112/SI95-122.1.

Navasakthi, S., Pandey, A., Dandautiya, R., Hasan, M., Khan, M.A., Perveen, K., Alam, S., Garg, R.Qamar, O., 2023. Assessment of spatial and temporal variation in water quality for the Godavari River. *Water* 15(17), 3076. https://doi.org/10.3390/w15173076.

Pattan, J.N., Pratibhan, G., Babu, C.P., Khadge, N.H., Paropkari, A.L., Kodagali, V.N., 2008. A note on geochemistry of surface sediments from Krishna-Godavari basin, East Coast of India. *J Geol. Soc. India* 71(1), 107–114.

Piper, A.M., 1944. A graphic procedure in the geochemical interpretation of water analyses. *Transactions of the American Geophysical Union* 25(6), 914–923. https://doi.org/10.1029/TR025i006p00914.

Pradhan, P.K., 1988. Birth of a fresh water lake from the Bay of Bengal. *Records of Geological Survey of India* 116(3-8), 87–95.

Ramana Murty, M.V., Rao, R.S., Bhagavan, S.V.B.K., 1993. Geomorphological studies for disaster mitigation—a case study of the Krishna Delta. *Andhra Pradesh, India. Int. J Remote Sensing* 14(17), 3269–3274. https://doi.org/10.1080/01431169308904441.

Rao, K.K., 1992. Evolution of Godavari Delta during Quaternary. *Records of Geological Survey of India* 125, 219–221.

Rao, K.N., Subraelu, P., Nagakumar, K.C.V., Demudu, G., Malini, B.H., Rajawat, A.S., 2013. Geomorphological implications of the basement structure in the Krishna-Godavari deltas, India. *Zeitschrift für Geomorphologie* 57(1), 25–44. https://doi.org/10.1127/0372-8854/2012/0076.

Rao, N.S., Subrahmanyam, A., 2017. Geochemical evolution of groundwater in the Western Delta region of River Godavari, Andhra Pradesh, India. *Applied Water Science* 7(2), 813–822. https://doi.org/10.1007/s13201-015-0294-y.

Reddy, K.M., Singaraju, V., 1989. Quaternary Geology and Geomorphology of the area around Goguleru Creek. near Bantumilli in Krishna District. *Records of Geological Survey of India* 122, 13–15.

Rengamannar, V., Dashora, S., 1989. Quaternary Geology and Geomorphology of coastal tracts in East Godavari district, Andhra Pradesh. *Records of Geological Survey of India* 122, 1–3.

Srinivas, B., Sarin, M.M., Sarma, V.V.S.S., 2011. Atmospheric dry deposition of inorganic and organic nitrogen to the Bay of Bengal: Impact of continental outflow. *Marine Chemistry* 127(1-4), 170–179. https://doi.org/10.1016/j.marchem.2011.09.002.

Tarawneh, M.S.M., Janardhana, M.R., Ahmed, M.M., 2019. Hydrochemical processes and groundwater quality assessment in North eastern region of Jordan valley, Jordan. *HydroResearch* 2, 129–145. https://doi.org/10.1016/j.hydres.2020.02.001.

WHO, 1996. *Guidelines for Drinking Water, v.2, Recommendations*. World Health Organization, Geneva.

Xu, D., Li, P., Chen, X., Yang, S., Zhang, P., Guo, F., 2023. Major ion hydrogeochemistry and health risk of groundwater nitrate in selected rural areas of the Guanzhong Basin, China. *Human and Ecological Risk Assessment.: An International Journal* 29(3-4), 701–727. https://doi.org/10.1080/10807039.2022.2164246.

